Reliability Assessment of Electronic Packaging with Hybrid Approach of Experimental and Computational Mechanics

Soon-Bok Lee[1]*and Ilho Kim[1]

[1] *School of Mechanical, Aeronautics, and System Engineering, Korea Advanced Institute of Science & Technology, 373-1 Guseong-dong, Yuseong-ku, Daejeon, 305-701, Korea*
e-mail: sblee@kaist.ac.kr, seamark@kaist.ac.kr

Abstract As electronic devices and components get smaller and faster in its speed, the package of the microelectronics rapidly changed to high density configuration of short pitch distance and small interconnection size and chip stacking. Consequently direct measurement of strain on electronic package become very difficult yet the reliability assessment of microelectronics packages become critical issue. Some optical methods are successfully adapted to measure the deformation, but there are many restrictions such as limited resolution of the experimental methods, unable to use in complex geometry. Moreover stress could not be obtained through optical method, because various materials in packages obstruct the converting optical-measured strain to stress. To assess the reliability of complex electronic packages, computational mechanics can provide the useful information that experimental mechanics can not provide. So the finite element analysis can be a powerful tool to assess the reliability of the advanced electronics packages. The accuracy of the results by computational mechanics, however, strongly depends on the material properties and the boundary condition.
This paper shows the procedure of reliability assessment for electronic packages, the hybrid approach of experimental and computational mechanics. First step is to create the reliability evaluation test suitable for the packages. Next step is to perform the simulation of stress/strain or deformation distribution using finite elements analysis. Finally, results of the test and the simulation are compared and correlated to get a damage parameter. In this study, two types of fatigue tests were conducted. First, cyclic bending tests were performed using the micro-bending tester. Second, thermal fatigue tests were conducted using a pseudo power cycling machine which was newly developed for a realistic testing condition. Two compositions of solder are tested in all test conditions, one is lead-free solder (95.5Sn4.0Ag0.5Cu) and the other is eutectic lead-contained solder (63Sn37Pb). A three-dimensional finite element analysis model was constructed. Computational analysis using ABAQUS was performed to extract the applied stress and strain in the solder joints. A constitutive model which includes both creep and plasticity was employed. From FEA results, the portion of the creep and plastic deformation are compared between the cyclic bending and thermal cycling tests. Lastly, the life prediction models are proposed.

Key words: reliability, FEA, lead-free, power cycling test, bending test

INTRODUCTION

Nowadays, the time to developing new type package is very important due to the life cycle of electronic products are getting shorter. Fast developing time of new electronic products generally yields more profit in markets. Therefore engineers who design the electronic package are interested in the method to reduce the developing time of packages. Computational mechanics with finite element method gives a power tool to evaluate the reliability of electronic packages. In reliability assurance of electronic packaging, one need to know the meaningful parameters such as stress, plastic strain, inelastic energy dissipation. The measuring methods and procedure to obtain stress and strain for large structures are well constructed and arranged on the standard books such as ASTM [1]. But, for the small structure such as electronic package, there are no suitable method to directly measure the stress and strain.
Recently, the optical method is in the limelight. The optical method gives the whole field image with high resolution without direct contacts on the surface[2]. If the measuring devices were in contact with the

specimen, there are relatively large error in the small structure. In spite of these benefit, the optical method has limitation. Moiré, Fizeau and Twyman-Green interferometers measure the surface displacement. To measure the inner points, the specimens should be sectioned, but that induces distortion because the boundary conditions have been changed. Additionally, the lamination structure restricts the converting measured displacement to stress.
One can reduce the developing time of electronic packaging and devices with computational method since finite element analysis can provide various engineering parameters necessary to developing electronics packaging. Finite element analysis can provide damage parameters required for applying on Coffin-Manson or Morrow models and also the stress and strain distributions of the package. Moreover the candidate designs could be compared with small cost and time because FEA can reduce the number of trial prototype devices. But FEA also has some drawbacks since FEA results highly depend on the inputs, such as material properties, boundary condition and quality of mesh configuration. If one of inputs is not reasonable, the results are not accurate too. The computational approach with aid of experimental support can provide a reasonable engineering solution for structural reliability of electronic devices.
The structural reliability of electronics devices was evaluated from the life prediction models. The life prediction models represent the relationships between cycles to failure and damage parameter. In this research, the life prediction models are made from the experimental obtained cycles to failure and computationally obtained damage parameters. In the life evaluation test for small electronic package, the damage parameters could not be measured directly, so the damage parameters are calculated from the finite element analysis which are simulated real testing. The inelastic equivalent strain and the inelastic energy dissipation are selected and compared as damage parameters.

EXPERIMENT - THERMAL CYCLING TESTS

Thermal fatigue tests were conducted with a pseudo-power cycling machine, which gives more realistic testing condition with high efficiency. Generally the power-cycling test requires power (heating) chip and a precise control technique [3-4]. And the chamber-cycling test has many shortages, as the package and PCB suffer isothermal condition and that required long testing time. To overcome the power- and chamber-cycling testing method, the pseudo-power cycling test method was proposed [5]. During the pseudo-power cycling, heat is transferred by conduction that could reduce the temperature rising and cooling times, which decrease the overall thermal cycling time.
A schematic view and a real photograph of the pseudo-power cycling machine are presented at Fig. 1(a) and (b). The temperatures of package and PCB and daisy chained resistance were measured in real-time. A personal computer controls the signals of heater and coolant automatically and records measured data concurrently. Detail descriptions on the pseudo-power cycling test method are listed elsewhere [6-7].

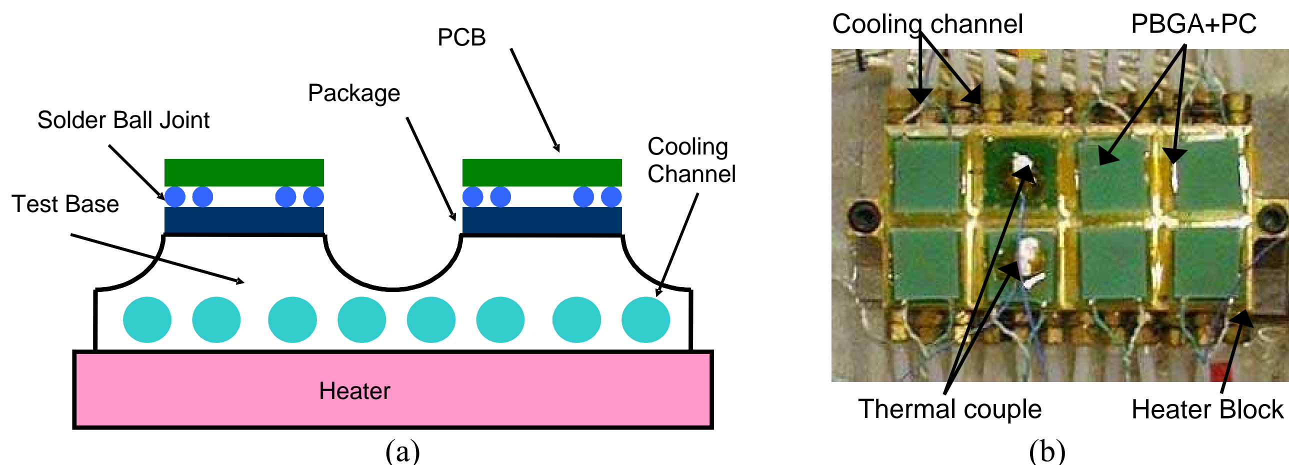

Fig. 1. (a) Schematic view and (b) A photograph of pseudo-power cycling machine.

Table 1. Conditions of thermal cycling test

63Sn37Pb	95.5Sn4.0Ag0.5Cu
30~150 ºC 30~125 ºC 30~110 ºC 30~100 ºC 30~75 ºC	30~150 ºC 30~130 ºC 30~110 ºC 30~100 ºC 30~90 ºC 30~70 ºC

Table 2. Time period of thermal cycling test

Total cycle time	7.5 min
Heating time	3 min
Holding time	3 min
Cooling time	1.5 min
Cycles per day	196 cycles

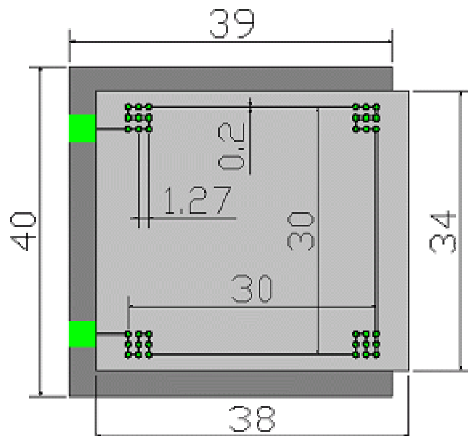

Fig. 2. Dimensions of thermal cycling test specimen.

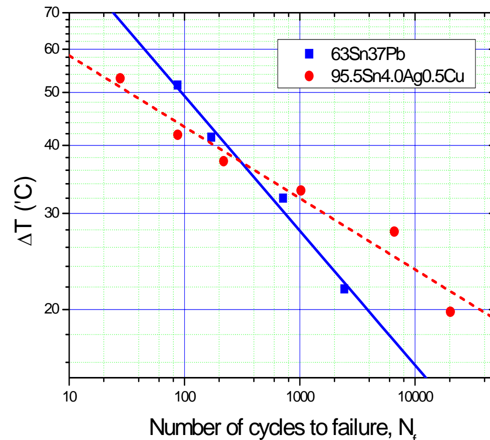

Fig. 3. ΔT versus thermal fatigue life curve.

Tested specimen was shown as Fig. 2. Two identical FR-4 PCBs of 2.0mm thickness were bonded by 36 solder joints, where 9 solder joints were laid on each corner. A lower PCB (white gray part at the Fig.2) is 40mm by 39mm and a upper PCB (dark gray part in the Fig.2) is 38mm by 34mm. The diameter of solder joints is 760μm and the pitch of solder joints is 1.27mm. For failure detection, a daisy-chain is constructed. The specimen has a large size and small number of solder ball joints, which makes the package weaker than conventional one. Because the large size induces large thermal expansion mismatch between upper and lower PCB and small number of solder joints means that each solder joint is subjected to more stress under the same CTE mismatch. As a result, an acceleration test is possible. The specimens are just placed on the top of the 'Test Base'. Thermal grease was applied to the contact surface of 'Test Base' to increase the conductivity between the 'Test Base' and package. It has enough viscosity to maintain the contact between package and the top surface of 'Test Base'. The testing conditions are listed on the Tables 1 and 2. Failure is defined when the resistance of the daisy chain exceeds 0.6Ω . Initial resistance of the daisy chain was 0.35Ω of room temperature, and 0.48Ω at high temperature region (150ºC). Higher temperature causes the thermal expansion on copper traces, so their length became longer and their area is reduced, which leads to increase the resistance of daisy chain.
Pseudo-power cycling test results are arranged and summarized using Weibull distribution (detail data are shown in [6-7]). The relationship between thermal fatigue life and ΔT is described in the Fig. 3. There exists cross points between the lead-contained solder and the lead-free solders. In large ΔT regions lead-contained solder (63Sn37Pb) has a good fatigue resistance, but in small ΔT regions lead-free solder (95.5Sn4.0Ag0.5Cu) has a longer fatigue life. According to the result in Fig.3, the solder which exhibit a good reliability could be reversed defending on the testing conditions

EXPERIMENT - CYCLIC BENDING TESTS

In this research, a small size bending tester was used as shown in Fig. 4. In this testing system, the electromagnetic actuator with a computer aided controller applies the cyclic force to the specimen. And a high resolution loadcell and LVDT measure the applied force and the moving distance of the whole specimen. The 256PBGA package is adopted for the bending test. Fig.5 shows the bending specimen. The 256PBGA package has a 27×27×0.36mm substrate with a 10×10×0.3mm die and 1.17mm thick

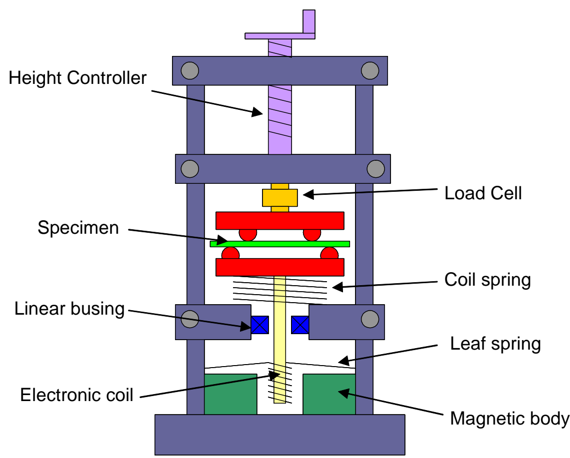

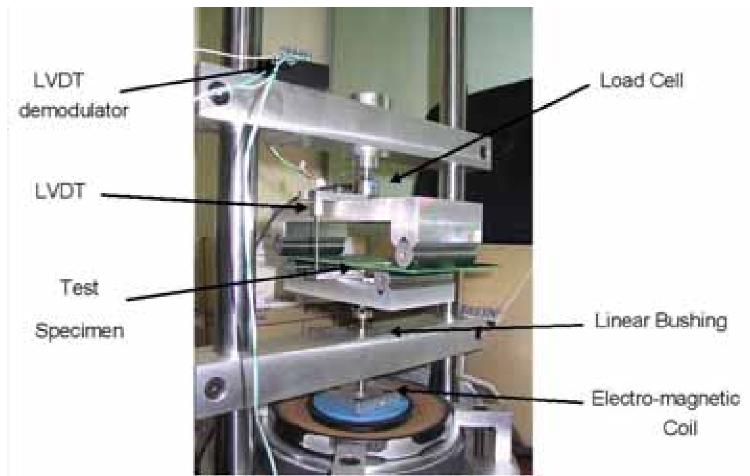

(a) (b)

Fig. 4. (a) Schematic view and (b) A photograph of four points micro-bending tester.

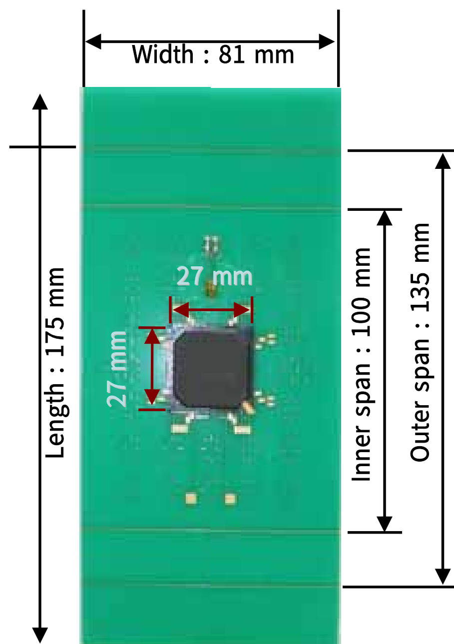

Fig. 5. Dimensions of thermal cycling test specimen.

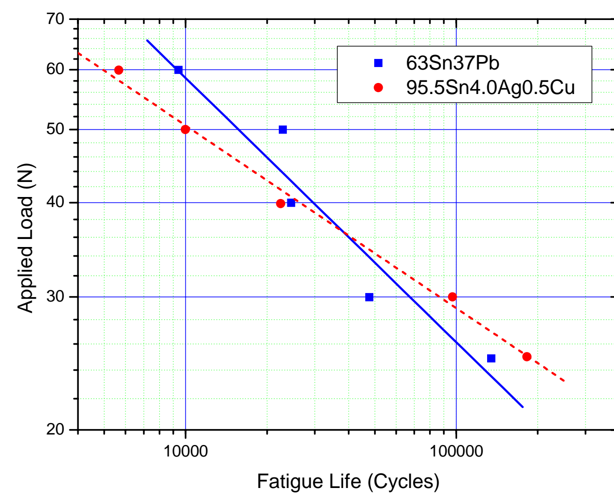

Fig. 6. Applied load versus fatigue life curve.

over-mold. There are 256 solder balls with 760㎛ diameter. The ball pitch is 1.27mm. There are two compositions of solder ball joints, one is eutectic lead-contained solder (63Sn37Pb), and the other is lead-free solder (95.5Sn4.0Ag0.5Cu). The PWB thickness was 1.0 mm and the pad diameter was 0.635 mm. The 256 PBGA and PWB were assembled to make test specimen via a reflow process in a nitrogen environment. Detail specifications of the bending tester and the specimen, and full explanation of the test results are shown elsewhere [8].

In this paper, brief summary is provided. Cyclic bending tests were performed using 1 Hz sinusoidal wave with various amplitudes ranging 25 to 60 N. Bending test results are described in the Fig.6. At each level, tests were repeated more than five times and the representative values were selected as the average. That result is similar to the thermal cycling test. Under high load conditions, lead-contained solders have longer fatigue life. On the contrary, lead-free solder sustain more cyclic loads under small load conditions. According to Figures 3 and 6, it can conclude that lead-free solder has good fatigue resistance in small load and lead-contained solder could sustain large loads.

FINITE ELEMENT MODEL

Finite element analysis using ABAQUS was performed to extract the applied stress and strain at the solder joints. For a precision drawing and good quality mesh, a three-dimensional finite element model was constructed from the modeling software Patran. Due to the symmetry, only one-eighth of the package was modeled for the thermal cycling specimen and a quarter was modeled for the cyclic bending specimen. For calculation efficiency, important solders were meshed finely, and the others were meshed coarsely from pre-FEA. The FE model for thermal cycling and cyclic bending tests were consisted with 20,962 elements (25,110 nodes) and 60,656 elements (75,343 nodes) respectively. Figs.7 and 8 show FE model of thermal cycling and cyclic bending tests, respectively. In thermal cycling model, package-side's temperature set to measured temperature and a convection coefficient of heat transfer was calculated to meet the measured temperature of PCB side. In cyclic bending model, loading rod is modeled as an analytical rigid body whose shape was calculated from a mathematical equation.

All of these FE models were made to have same mesh size and shape, because generally the FE analysis results depend on the mesh size and shape. The material properties of the models are obtained from website and Park, Hong and Lau's works [9-12] where creep properties of 95.5Sn3.9Ag0.6Cu is selected for 95.5Sn4.0Ag0.5Cu solder due to the lack of available material data. A constitutive model including both creep and plasticity was employed. And some properties whose temperature dependency is critical were described to reflect that effect. Adopted material models are listed in Table 3 and 4.

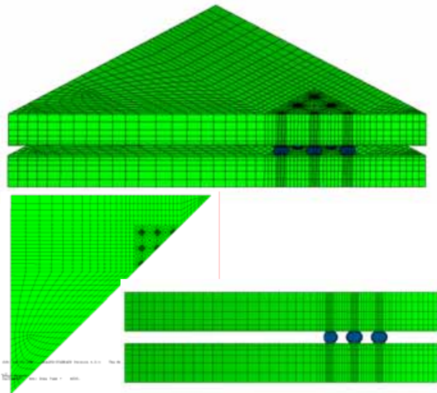

Fig. 7. FE model for thermal cycling test.

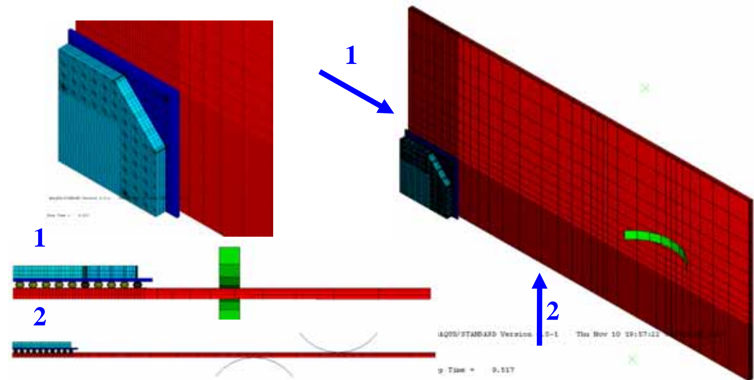

Fig. 8. FE model for cyclic bending test.

Table 3. Material Properties for finite element analysis

	Temperature (K)	Density (kg/m^3)	Specific Heat	Thermal Conductivity (W/mK)	CTE (ppm/K) (X,Y/Z)	Elastic Modulus (MPa)	Poisson Ratio	Yield Strength (MPa) Strain(0/0.01/0.1)
Lead-contained Solder	278 323 373 398	8470	150	51	25.2 26.1 27.3 37.9	44377 41334 36854 34586	0.36 0.365 0.3774 0.3839	29.86 22.96 12.31 9.35
Lead-free Solder	298 343 373	7400	226	33	21.3 22.15 23	53000 47000 44000	0.4	30/45/180 23/29/83 18/20/38
FR-4	273 338 450	1938	879	10	19/70 19/98 19/179	22000 (X,Y) 11000 (Z)	0.11 (X,Y) 0.28 (Z)	elastic
Copper	-	8942	385	389	16.7	117000	0.34	69.0
Epoxy	228 383	1699	2093	0.2	6.68 10.5	29300 23000	0.35 0.35	elastic
Silicon	273 323 373	2330	687	83.7	2.8729 3.0764 3.411	130194 129809 120382	0.2783 0.2781 0.278	elastic

Table 4. Creep properties for finite element analysis.

Creep behavior $\dot{\varepsilon} = A[\sinh(B\sigma)]^n \exp\left(-\frac{Q}{RT}\right)$				
	A(1/s)	B(1/MPa)	n	Q(J/mole)
63Sn37Pb	12423	0.126	1.89	61417
95.5Sn4.0Ag0.5Cu	44100	0.005	4.2	44995

MATERIAL BEHAVIOR OF SOLDER JOINTS

There are two mechanisms to induce solder joints failure. One is creep mechanism. The materials used for soldering has low melting temperature, that means the homologous temperature is high even at room temperature. Therefore a lot of creep was occurred during the thermal cycling test. Another major failure mechanism is plastic deformation. Specially, bending force induce relatively higher plastic deformation. In this research, the portions of two different failure mechanisms were compared. Figs.9 and 10 show the energy dissipation during cycling tests. The energy dissipation was calculated from

$$E = \sum_{i=1}^{n} W_i V_i \tag{1}$$

where energy E, energy density W and volume V is in J, J/m^3, m^3, respectively. And n is the number of interest elements. For convenience, dissipation energy and dissipated energy density per cycle are designated as E and ΔW, respectively. And the subscript "cr", "pl" and "in" represent the creep, plastic and inelastic (total) energy, respectively. ΔW means that the volume averaged increase of E during one cycle on the stable cycles. ΔW was calculated from

$$\Delta W = \frac{\sum_{i=1}^{n} dE_i}{\sum_{i=1}^{n} V_i} \tag{2}$$

where dE is increase of E during a cycle at a stable stage. For the exact analysis, E_{cr} and E_{pl} are distinguished from E_{in}. FE analysis was conducted until 30 cycles for cyclic bending and thermal cycling tests. Because the enough time is needed to stabilize ΔW.

In the thermal cycling tests, E_{cr} is larger than E_{pl}, at all of the cases as shown in Fig.9. As thermal load is increased, the E_{cr} and E_{pl} increased, especially E_{cr} is prominent. The E_{pl} is saturated after 10~20 cycles, but, E_{cr} increases almost linearly from the initial cycle. The ΔW_{cr} is about 40 to 90 times larger than ΔW_{pl}.

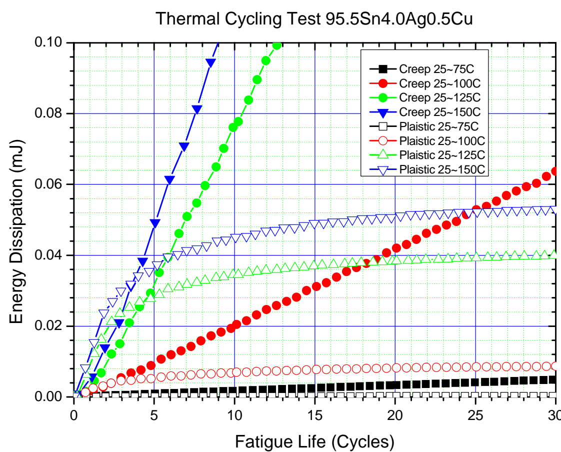

Fig. 9. Energy dissipation on thermal cycling tests.

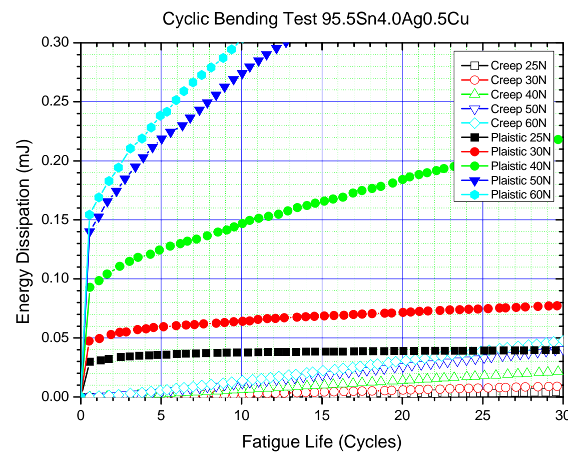

Fig. 10. Energy dissipation on cyclic bending tests.

These facts mean that plastic deformation, which occurred in early stage, was disappeared on stable stage. On the contrary, ΔW_{pl} is about 2 to 7 times larger than ΔW_{cr} in cyclic bending tests (see Fig.10). For the 1~26 N loading case, ΔW_{cr} is about 2 times larger, even if E_{pl} is larger than E_{cr} as shown in the Fig.10. On the 1~26N case, large plastic deformation occurred in early stage, and then an increase rate of plastic deformation suddenly decreased. Therefore, ΔW_{cr} is larger at the cyclic stable stage. The ratio of ΔW_{pl} to ΔW_{cr} increases as the applied load increases. On high load test condition (over 30N), E_{pl} is not saturated and is accumulated as a damage. From Figs. 9 and 10, there is the distinction between the major energy dissipation mechanisms on thermal and bending test, and it could be found that creep is principal damage in thermal cycling test and plasticity is essential damage in cyclic bending test.

LIFE PREDITION MODEL

There are many types of fatigue life prediction models. Typically, strain- and energy- damage based models are used for solder. Figs. 11 and 12 show the relationships between the inelastic equivalent strain increase ($\Delta\varepsilon_{in}^{eq}$) and fatigue life($N_f$) for lead-free and lead-contained solder, respectively. The inelastic equivalent strain is calculated from Eq. 3.

$$\Delta\varepsilon_{in}^{eq} = \int_0^t \left(\sqrt{\frac{2}{3}\dot{\varepsilon}_{cr} : \dot{\varepsilon}_{cr}} + \sqrt{\frac{2}{3}\dot{\varepsilon}_{pl} : \dot{\varepsilon}_{pl}} \right) dt \quad (3)$$

The strain distribution of solder joint is very complex. In order words, each point on the solder joint has different strain. In this study, the element showing the maximum strain is selected to the representative one. The correlation between inelastic energy dissipation density per cycle (ΔW_{in}) and fatigue life(N_f) is depicted in Figs. 13 to 16. For a general use, volume normalized value ΔW_{in} is substituted for ΔE_{in}. Energy dissipation on each element depends also on the position of solder joints. Therefore ΔW_{in} could be changed according to number of elements averaged for representative ΔW_{in}[13]. In this study, ΔW_{in} is averaged to two different volumes, one is whole solder joint and another is the interface elements, which the crack is propagated. The ΔW_{in} on whole solder joints is more convenience to correlate with experimental data, because the interface's dissipation energy could not be measured experimentally. However from observation on failure phenomena, the failures of solder ball joints are induced by the interface crack propagation, since the barrel shape of solder joint makes stress concentration on the interface between the solder joint and package or PCB. The ΔW_{in} on interface can be more reasonable and a critical damage parameter, however ΔW_{in} of interface could not be measured experimentally and only calculated using FEA.

In Figs. 11 to 16, the predicted lives are also depicted as white rectangles for cyclic bending test and white circles for thermal cycling tests using the Eq. 4 to 9. Eqs. 2 and 3 represent the modified Coffin-Manson's strain-based life prediction model. Eqs. 4 to 9 show the modified Morrow's energy-based life prediction model. These models were modified with active energy concept to include temperature effects. These models were constructed with the following procedure. First, the exponent of damage parameter is decided from the cyclic bending test results with the assumption that slope does not change on the temperature. In the cyclic bending test results, there are no temperature effects, because the cyclic bending tests were performed on the room temperature. Second, the effective temperatures are set to $0.75T_{max}$. Total dissipation energy until failure depends on the temperature. As temperature increases, total dissipation energy decreases with higher rate. So, effective temperature was set to $0.75T_{max}$ with considering the effect of higher temperatures. Third, activation energy and constants were found using least-square method.

In the lead-free material, life prediction model using $\Delta\varepsilon_{in}^{eq}$ as damage parameter (Eq. 4) has minimum error between measured life and predicted life. But in the lead-contained solder, strain-based models (Eq.5) take larger error than others. The accuracy of two different energy based models is similar on two solder compositions.

$$N_f = 6.216 \times 10^{-9} \Delta\varepsilon_{in}^{eq\,-0.990} e^{\frac{63277}{8.314 \times T}} \quad : \text{SnAgCu} \quad (4)$$

$$N_f = 1.238 \times 10^{-8} \Delta\varepsilon_{in}^{eq\,-1.36728} e^{\frac{63642}{8.314 \times T}} \quad : \text{SnPb} \quad (5)$$

$$N_f = 1.519 \times 10^{-5} \Delta W_{in}^{-0.840} e^{\frac{43669}{8.314 \times T}} \quad \text{: SnAgCu whole-elements averaged} \tag{6}$$

$$N_f = 7.121 \times 10^{-7} \Delta W_{in}^{-1.111} e^{\frac{51646}{8.314 \times T}} \quad \text{: SnPb whole-elements averaged} \tag{7}$$

$$N_f = 2.306 \times 10^{-6} \Delta W_{in}^{-0.835} e^{\frac{55353}{8.314 \times T}} \quad \text{: SnAgCu interface-elements averaged} \tag{8}$$

$$N_f = 3.293 \times 10^{-5} \Delta W_{in}^{-1.111} e^{\frac{51652}{8.314 \times T}} \quad \text{: SnPb interface-elements averaged} \tag{9}$$

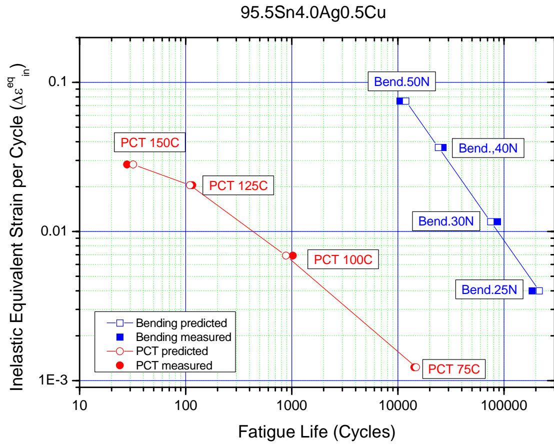

Fig. 11. $\Delta\varepsilon^{eq}_{in}$ vs. N_f curve for lead-free solder.

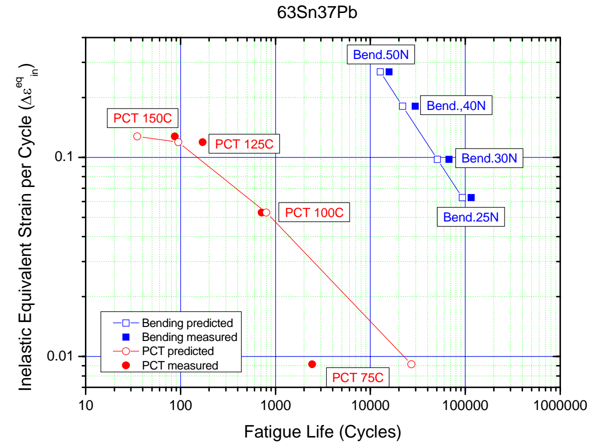

Fig. 12. $\Delta\varepsilon^{eq}_{in}$ vs. N_f curve for lead-contained solder.

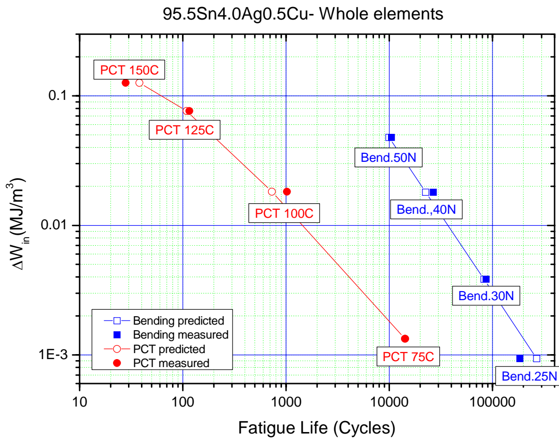

Fig. 13. ΔW_{in}^{wh} vs. N_f curve for lead-free solder.

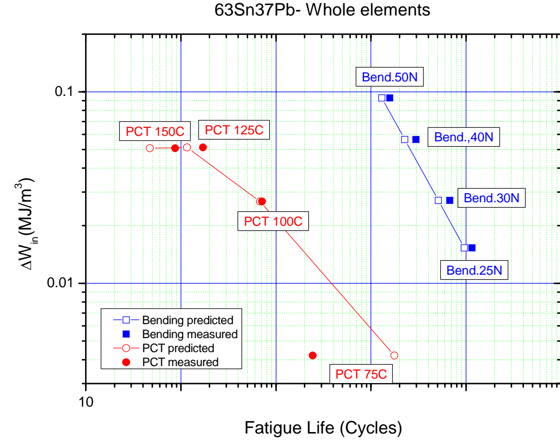

Fig. 14. ΔW_{in}^{wh} vs. N_f curve for lead-contained solder.

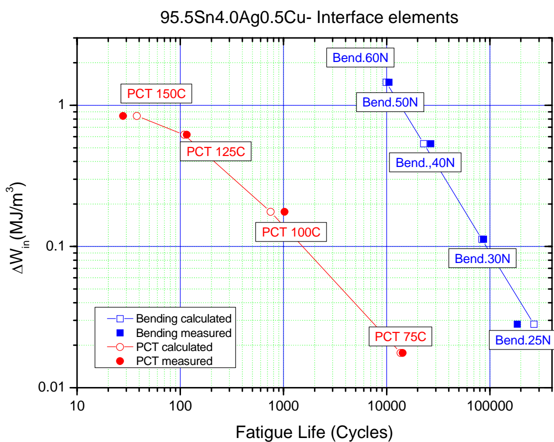

Fig. 15. ΔW_{in}^{it} vs. N_f curve for lead-free solder.

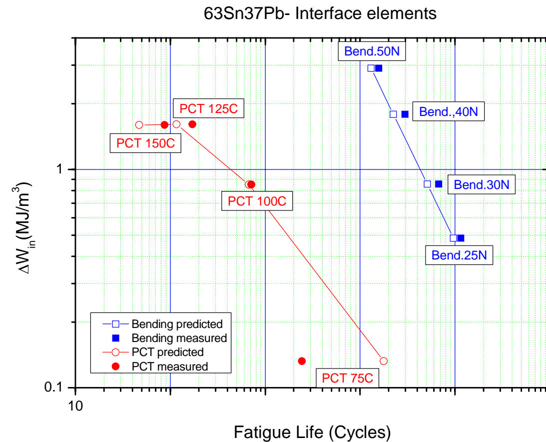

Fig. 16. ΔW_{in}^{it} vs. N_f curve for lead-contained solder.

CONCLUSION

In this paper, two energy-based models and a strain-based model were proposed for lead-free and lead-contained solder. Those life prediction models are constructed from experimental data and FEA. Fatigue life data are acquired from the thermal cycling test and cyclic bending test and damage parameters are calculated through the FEA, which simulate thermal cycling test and cyclic bending test. In the thermal cycling test, the creep deformation is dominant, but in the cyclic bending test the portion of plastic deformation is higher. The fatigue life of cyclic bending test shows linear relationship with damage parameters such as inelastic strain and dissipation energy, but the fatigue life acquired from thermal cycling test has non-linear relationship due to the thermal degradation. The thermal degradation was modeled as Arrhenius type equation and showed a good agreement with data.

ACKNOWLEDGEMENTS

This work was supported by Ministry of Science and Technology in Korea through “Development of Reliability Design Technique and Life Prediction Model for Electronic Components”.

REFERENCES

[1] *Annual book of ASTM Standards*, American Society for Testing and Materials, West Conshohocken.

[2] D. Post, B. Han, P. Lfju *High Sensitivity Moiré* , Springer-Verlag, New York (1994).

[3] S. Wen, et al, *Fast Power-Cycling Test of Area-Array Interconnected Power Devices*, Annual power electronics seminar (2002), pp.456-462.

[4] J. Lenkkeri, et al, *Rapid power cycling of flip-chip and CSP components on ceramic substrates*, Microelectronics Reliability, vol. 41, (2001), pp661-668.

[5] T. S. Park, *A Study for Reliability Assurance of Surface Mount Component Through Thermal Fatigue Testing*, Master’s Thesis, MME98037, KAIST, Daejeon (1998).

[6] I. Kim, *A Study on Thermal Fatigue Behavior of BGA Package*, Master’s Thesis, MME04018, KAIST, Daejeon (2004).

[7] I. Kim, et al, *A Comparative Study of The Fatigue Behavior of SnAgCu and SnPb Solder Joints*, Key Engineering Materials, Vols. 297-300 (2005), pp.831-836.

[8] I. Kim, S.-B. Lee, *Reliability Assessment of BGA Solder Joints under Cyclic Bending Loads*, in *Proc. 7th Int. Conf. on Electronic Materials and Packaging 2005*, Tokyo, Japan (2005).

[9] website, www.matweb.com

[10] T. S. Park, *A study on mechanical fatigue behaviors of ball grid array solder joints for electronic packaging*, Doctoral thesis, DME 04041, KAIST, Daejeon (2004).

[11] B.Z. Hong, *Thermal fatigue analysis of a CBGA package with lead-free solder fillets*, in *Proc. InterSociety Conference on Thermal Phenomena* (1998), pp. 205-211.

[12] J. Lau, et al, *Acceleration models, constitutive equations, and reliability of lead-free solders and joints*, in *Proc. 53th Electronic Components and Technology Conf.*, New Orleans Louisiana (2003), pp. 229-236.

[13] B.A. Zahn, *Solder Joint Fatigue Life Model Methodology for 63Sn37Pb and 95.5Sn4Ag0.5Cu Materials*, in *Proc. 53th Electronic Components and Technology Conf.*, New Orleans Louisiana (2003), pp. 83-94.

[14] P. Towashiraporn, et al. *Power cycling thermal fatigue of Sn-Pb solder joints on a chip scale package*, International Journal of Fatigue, Vol. 26 (2004), pp.497-510.